J. Fluid Mech. (1985), *vol.* 152, *pp.* 15–38
Printed in Great Britain

Slow-zone model for longitudinal dispersion in two-dimensional shear flows

By S. C. CHIKWENDU
Mechanical Engineering Department, University of Nigeria, Nsukka

AND G. U. OJIAKOR
Civil Engineering Department, University of Nigeria, Nsukka

(Received 2 December 1983 and in revised form 27 June 1984)

A two-zone model is proposed for the longitudinal dispersion of contaminants in two-dimensional turbulent flow in open channels – a fast zone in the upper region of the flow, and a slow zone nearer to the bottom. The usual one-dimensional dispersion approach (Elder 1959) is used in each zone, but with different flow speeds U_1 and U_2 and dispersion coefficients D_1 and D_2 in the fast and slow zones respectively. However, turbulent vertical mixing is allowed at the interface between the two zones, with a small vertical diffusivity ϵ. This leads to a pair of coupled, linear, one-dimensional dispersion equations, which are solved by Fourier transformation. The Fourier-inversion integrals are analysed using two different methods.

In the first method asymptotically valid expressions are found using the saddle-point method. The resulting cross-sectional average concentration consists of a leading Gaussian distribution followed by a trailing Gaussian distribution. The trailing Gaussian cloud disperses (longitudinally) faster than the leading one, and this gives the long tail observed in most dispersion experiments. Significantly the peak value of the average concentration is found to decay exponentially with time at a rate which is close to the rate observed by Sullivan (1971) in the early stage of the dispersion process. The solution is useful for fairly small times, and both the calculated value of D_1 and the predicted bulk concentration distribution are in meaningful agreement with the experimental and simulation data of Sullivan (1971).

In the second method an exact solution is found in the form of a convolution integral for the case $D_1 = D_2 = D_0$. Explicit expressions which are valid for small times and for large times from the release of contaminant are found. For small times this exact solution confirms the basic results obtained by the saddle-point method. For large times the exact solution gives a contaminant concentration which approaches a Gaussian distribution travelling with the bulk speed as predicted by the Taylor model. The overall longitudinal dispersion coefficient at large times, $D(\infty)$, consists of the diffusivity D_0 plus a contribution $D_\ell(\infty)$ which depends entirely on the vertical mixing. $D(\infty)$ is in good agreement with Chatwin's (1971) interpretation of Fischer's (1966) experimental data.

1. Introduction

The study of longitudinal dispersion in shear flows was pioneered by Taylor (1953, 1954), who showed that the dispersion of dissolved or suspended matter in laminar or turbulent pipe flow can be modelled by a one-dimensional advective–diffusion

equation. His method has been extended to two- and three-dimensional turbulent flows in open channels and streams by Elder (1959), Aris (1956), Fischer (1966) and others. Much research work continues on such questions as better prediction of the longitudinal dispersion coefficients, the effect of the viscous sublayer, vertical and lateral dispersion coefficients, dispersion in estuaries, and other problems.

One problem is the fact that the one-dimensional model always predicts a normal distribution of matter down the channel for all time, whereas observed distributions of dispersing clouds are always skewed, especially at small times. Sullivan (1971) used a three-stage model to explain this skewness. In the first stage, referring to the period of time shortly after the release of the contaminant, the upper layer $y > \frac{1}{2}h$ is well mixed, while there is no significant flux of contaminant from this layer to the lower layer $y < \frac{1}{2}h$, which moves more slowly (here h is the depth of the flow and y is the vertical distance from the bottom of the channel). In the second stage, referring to later times, the upper layer consists of the region $y > y^+$, where y^+ is the thickness of the viscosity-dominated layer. In the third stage, referring to large times, the entire flow depth is one layer. Sullivan used statistical simulation to show the validity of his description, especially in the first stage.

Some other researchers have used two-layer models to study various aspects of the dispersion process. Hays (1966) developed a dead-zone model to describe the effects of regions of stagnant fluid (dead zones) in streams. Chatwin (1973) used two layers (the mainstream and the viscosity-dominated layer) having a linear velocity profile and calculated some effects of the viscous layer on turbulent dispersion. Thacker (1976) showed that for a flow with two equal layers, each of which is well-mixed and has negligible horizontal diffusivity ($D_1 = D_2 = 0$), the bulk concentration satisfies a telegraph equation. He thus obtained an exact analytic solution for this non-diffusive case, and also touched briefly upon the diffusive case $D_1 = D_2 \neq 0$. Smith (1981, 1982) has also studied a delay–diffusion description that is equivalent to the two-layer model, and also used the telegraph equation to obtain exact solutions for the non-diffusive case $D_1 = D_2 = 0$. He also showed how the layers should be chosen so as to achieve good results.

This paper proposes a partial-differential-equation approach to explain the skewed profile by means of a two-zone model. The flow is divided into a fast zone and a slow zone which interact while each zone is governed by a linear one-dimensional dispersion equation. This idea was conceived because of the experimental observation that most turbulent shear flows consist of a centre or surface section of approximately uniform velocity, and rapid velocity gradients near the boundaries. Thus our model consists of a slow-moving zone near the *bottom and sides* of the channel and a fast-moving zone in the middle of the channel. We assume that each zone is well mixed and thus has a uniform concentration of contaminant, while turbulent diffusion takes place at the interface between the two zones, leading to coupling of the governing equations.

It should be noted that Elder (1959) suggested that the skewed distribution could be discussed in two parts: a forward Gaussian distribution representing contaminant over the major part of the cross-section, and a second Gaussian distribution representing dyed fluid in the viscous layer. This paper thus provides a detailed mathematical model of Elder's suggestion and Sullivan's (1971) description, where the slow layer is here interpreted as the region of rapid turbulent velocity gradient near the boundaries (and not the viscosity-dominated layer).

In our asymptotic solution it is important that D_1 and D_2 are non-zero, while the vertical diffusion coefficient ϵ is small. This makes it possible for us to apply

perturbation expansions in powers of ϵ. It is also important that $D_2 > D_1$, as this makes it possible for the contaminant to disperse faster in the slow zone than in the fast zone (at small times), thus giving the characteristic long tail. However, the exact solution analysed in §§8–11 for the case $D_1 = D_2$ gives significant results both for small times and for large times.

2. Derivation of coupled slow- and fast-zone equations

Although the basic idea of the slow-zone model can be applied to three-dimensional open-channel flow and to pipe flow, the derivation and the solution of the equations in this paper will be concerned with the case of turbulent two-dimensional open-channel flow. Thus we assume that the channel is sufficiently wide such that the dispersion of matter in the flow will be governed by the two-dimensional diffusion equation

$$\partial_t c = D_{\mathrm{L}} \partial_x^2 c + D_{\mathrm{V}} \partial_y^2 c - u(y) \partial_x c, \tag{2.1}$$

where c is the concentration of contaminant, x and y are respectively the downstream longitudinal and vertical Cartesian coordinates in the channel, D_{L} and D_{V} are respectively the turbulent longitudinal and vertical dispersion coefficients, u is the fluid velocity (independent of x) and t is the time.

Consider the fast and slow zones shown in figure 1. Equation (2.1) can be averaged over the cross-sectional area of each zone (in the manner of Elder 1959), leading to two different one-dimensional dispersion equations, one in each zone. However, through the vertical-diffusion term in (2.1), we shall take into account the vertical turbulent diffusion at the interface between the two zones. This will be done in the same way as Hays (1966) did for his dead-zone model.

Let h_1 and h_2 be the thicknesses of the fast and slow zones respectively. We assume that each zone is well mixed, with cross-sectional averages c_1, c_2 and u_1, u_2 for the contaminant concentrations and velocities in the fast and slow zones respectively. The mass flux of contaminant by turbulent diffusion across the interface from the fast to the slow zone is thus

$$-M_{\mathrm{T}} = a(c_1 - c_2), \tag{2.2}$$

where a is a constant. This mass moves into the slow zone per unit time per unit area of the interface and contributes to the time rate of change of the concentration in the slow zone. A similar equation can be written for the transfer of mass from the slow to the fast zone:

$$M_{\mathrm{T}} = a(c_2 - c_1). \tag{2.3}$$

Thus, averaging (2.1) over the cross-section in each zone, the resulting coupled slow- and fast-zone advective–diffusion equations are

$$\partial_t c_1 = D_{1\mathrm{L}} \partial_x^2 c_1 - u_1 \partial_x c_1 + \frac{a}{h_1}(c_2 - c_1), \tag{2.4a}$$

$$\partial_t c_2 = D_{2\mathrm{L}} \partial_x^2 c_2 - u_2 \partial_x c_2 + \frac{a}{h_2}(c_1 - c_2), \tag{2.4b}$$

where $D_{1\mathrm{L}}$ and $D_{2\mathrm{L}}$ are the average longitudinal dispersion coefficients in the fast and slow zones respectively. If h is the depth of the flow in the channel then

$$h_1 + h_2 = h; \quad \frac{h_1}{h} = \eta_1; \quad \frac{h_2}{h} = \eta_2, \tag{2.5}$$

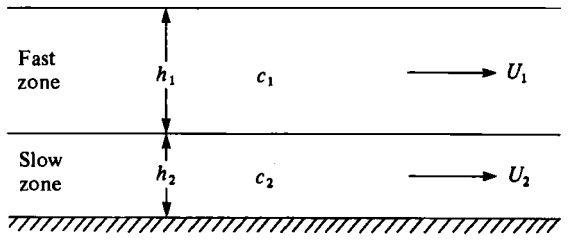

FIGURE 1. Channel, showing slow zone and fast zone.

where η_1 and η_2 are the fractional depths of the fast and slow zones respectively. We also define

$$\beta_1 = \frac{1}{\eta_1}; \quad \beta_2 = \frac{1}{\eta_2}.$$

If u_* is the friction velocity of the flow, it is convenient to non-dimensionalize the parameters in the coupled dispersion equations (2.4) by means of the following nondimensional variables and constants:

$$\left.\begin{aligned} X &= \frac{x}{h}, \quad U_1 = \frac{u_1}{u_*}, \quad U_2 = \frac{u_2}{u_*}, \\ T &= \frac{tu_*}{h}, \quad Y = \frac{y}{h}, \quad D_1 = \frac{D_{1L}}{hu_*}, \\ D_2 &= \frac{D_{2L}}{hu_*}, \quad \epsilon_V = \frac{D_V}{hu_*}, \quad \epsilon = \frac{a}{u_*}. \end{aligned}\right\} \tag{2.6}$$

The non-dimensionalized forms of (2.4) are thus

$$\partial_T c_1 = D_1 \partial_X^2 c_1 - U_1 \partial_X c_1 + \epsilon\beta_1(c_2 - c_1), \tag{2.7a}$$

$$\partial_T c_2 = D_2 \partial_X^2 c_2 - U_2 \partial_X c_2 + \epsilon\beta_2(c_1 - c_2). \tag{2.7b}$$

It may be noted that when $\beta_2 = \infty$ (i.e. when the slow zone has zero thickness) then $c_1 = c_2$ in (2.7*b*). The coupled equations (2.7) then reduce to the usual single one-dimensional dispersion equation.

Initial conditions of rapid injection

An important initial-boundary-value dispersion problem is that in which a mass of contaminant is rapidly injected or dumped at an initial location and subsequently disperses downstream. If the contaminant is assumed to be well mixed in the initial vertical layer, then the initial conditions for (2.7) are

$$c_1(X, 0) = c_2(X, 0) = c_0\,\delta(X), \tag{2.8}$$

where c_0 is the initial concentration of contaminant and δ is the Dirac delta function.

3. The constants of the model

The constants that appear in (2.7) are the longitudinal and vertical dispersion coefficients D_1, D_2 and ϵ, the average velocities U_1, U_2, and β_1, β_2, which are the inverses of the fractional depths.

3.1. *Velocity profile*

We shall assume that the flow velocity is given by von Kármán's logarithmic profile

$$u(Y) = \bar{u} + \frac{u_*}{\kappa}(1 + \ln Y), \tag{3.1}$$

where $Y = y/h$, $\bar{u}$ is the average velocity over the entire cross-section and κ is von Kármán's constant (about 0.4). For two-dimensional shear flow the validity of the logarithmic profile (away from the boundary) has been well established experimentally (e.g. Fischer 1966).

The depth ratio is

$$\eta = \eta_2/\eta_1 . \tag{3.2}$$

Thus the non-dimensionalized average velocity in the slow zone will be

$$U_2 = \frac{1}{\eta_2}\int_0^{\eta_2} \frac{u(Y)}{u_*}\,\mathrm{d}Y; \tag{3.3}$$

and using (3.1) in (3.3) and integrating gives

$$U_2 = U + \frac{1}{\kappa}\ln \eta_2, \tag{3.4a}$$

where $U = \bar{u}/u_*$ is the non-dimensional overall average velocity. Similarly, in the fast zone,

$$U_1 = \frac{1}{1-\eta_2}\int_{\eta_2}^{1} \frac{u(Y)}{u_*}\,\mathrm{d}Y,$$

or

$$U_1 = U - \frac{\eta}{\kappa}\ln \eta_2. \tag{3.4b}$$

It may be noted that

$$U = (1-\eta_2)\,U_1 + \eta_2\,U_2. \tag{3.4c}$$

3.2. *Estimates of the longitudinal and vertical dispersion coefficients*

For two-dimensional open-channel flow the theoretical formula obtained by Elder (1959) (also see Chatwin 1971, equation (5.2)) for the longitudinal dispersion coefficient is

$$D_{\mathrm{L}} = \frac{1}{h}\int_0^h \frac{1}{D_y}\mathrm{d}y\left[\int_0^y u'(y)\,\mathrm{d}y\right]^2, \tag{3.5a}$$

where

$$u'(y) = u(y) - \bar{u}, \quad D_y = hu_*\kappa y(1-y).$$

In dimensionless form, (3.5a) can be written as

$$D = \frac{D_{\mathrm{L}}}{hu_*} = \kappa^{-3}\int_0^1 \epsilon_y^{-1}\,\mathrm{d}Y\left[\int_0^Y U'(Y)\,\mathrm{d}Y\right]^2, \tag{3.5b}$$

where $\epsilon_y = Y(1-Y)$, $U'(Y) = u(Y)/u_* - U$.

If the method of Elder (1959) is applied to the slow zone, then, in a similar form to (3.5b), the resulting equation for D_2 is

$$D_2 = \kappa^{-3}\eta_2^{-1}\int_0^{\eta_2} \epsilon_y^{-1}\,\mathrm{d}Y\left[\int_0^Y U_2'(Y)\,\mathrm{d}Y\right]^2, \tag{3.6a}$$

where $U_2'(Y) = u(Y)/u_* - U_2$.

Similarly, in the fast zone the longitudinal dispersion coefficient obtained is

$$D_1 = \kappa^{-3}\eta_1^{-1}\int_{\eta_2}^{1}\epsilon_y^{-1}\,\mathrm{d}Y\left[\int_{\eta_2}^{Y}U_1'(Y)\,\mathrm{d}Y\right]^2, \tag{3.6b}$$

where $$U_1'(Y) = u(Y)/u_* - U_1.$$

After the integrals in the brackets have been evaluated, (3.6*a*,*b*) can be written as

$$D_2 = \kappa^{-3}\eta_2^{-1}\int_0^{\eta_2} Y(1-Y)^{-1}\left[\ln\frac{Y}{\eta_2}\right]^2\mathrm{d}Y, \tag{3.7a}$$

$$D_1 = \kappa^{-3}\eta_1^{-1}\int_{\eta_2}^{1} Y^{-1}(1-Y)^{-1}\left[Y\ln Y-(1-Y)\frac{\eta_2}{\eta_1}\ln\eta_2\right]^2\mathrm{d}Y. \tag{3.7b}$$

It will be shown in §11 that the optimal choice for the fractional depths of the zones gives

$$\eta_2 = \mathrm{e}^{-1} = 0.3679; \quad \eta_1 = 1-\mathrm{e}^{-1} = 0.6321.$$

Using these values of the fractional depths, the integrals in (3.7*a*,*b*) were evaluated numerically, and the resulting longitudinal diffusivities in the fast and slow zones found to be

$$D_1 = \frac{0.0164}{\kappa^3}; \quad D_2 = \frac{0.1033}{\kappa^3}. \tag{3.8a}$$

If $\kappa = 0.41$ it is found that

$$D_1 = 0.24, \quad D_2 = 1.50. \tag{3.8b}$$

For the vertical dispersion coefficient, the cross-sectional average value obtained by Elder (1959) is

$$D_{\mathrm{V}} = \tfrac{1}{6}\kappa h u_*, \quad \epsilon_{\mathrm{V}} = \tfrac{1}{6}\kappa \approx 0.067. \tag{3.9}$$

This approximate value was referred to by Fischer (1973) and has been confirmed by the experiments of Jobson & Sayre (1970).

In order to estimate the vertical diffusion rate a that appears in (2.2) and (2.4), consider the concentration profile shown in figure 2. The dotted line in figure 2 runs from the midpoint of the fast zone to the midpoint of the slow zone, and indicates that the average concentration gradient can be estimated to be

$$\frac{\partial c}{\partial y} \approx \frac{c_1 - c_2}{\frac{1}{2}h}. \tag{3.10}$$

Thus, if the vertical diffusion rate is D_{V} as in (2.1), then the mass flux will be given (in analogy with Fourier's law of heat conduction), by

$$M_{\mathrm{T}} = -D_{\mathrm{V}}\frac{\partial c}{\partial y}. \tag{3.11}$$

Combinning (2.2), (3.10) and (3.11), it is found that

$$-M_{\mathrm{T}} = a(c_1 - c_2) = \frac{2D_{\mathrm{V}}}{h}(c_1 - c_2). \tag{3.12}$$

Thus $$a \approx 2D_{\mathrm{V}}/h, \tag{3.13}$$

and, using (2.10) and (3.9), we find that

$$\epsilon \approx 2\epsilon_{\mathrm{V}} = \tfrac{1}{3}\kappa \approx 0.137. \tag{3.14}$$

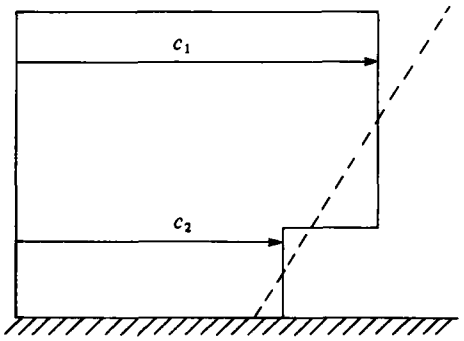

FIGURE 2. Concentration profile showing fast-zone (c_1) and slow-zone (c_2) contaminant concentrations. The dotted line indicates the average concentration gradient.

This value of ϵ is in agreement with the value of 0.12 found by Sullivan (1971) for the average non-dimensional lateral diffusivity as given in his table 2.

Thus ϵ is a fairly small parameter, and this fact will prove useful in our asymptotic analysis of the coupled dispersion equations (2.7).

4. Solution by Fourier transforms

We shall solve the coupled fast- and slow-zone equations (2.7) by Fourier transformation with respect to X, using the Fourier transforms

$$F_n(\lambda, T) = \int_{-\infty}^{\infty} e^{i\lambda X} c_n(X, T)\, dX, \quad n = 1, 2, \tag{4.1a}$$

and their inverses

$$c_n(X, T) = \frac{1}{2\pi} \int_{-\infty}^{\infty} e^{-i\lambda X} F_n(\lambda, T)\, d\lambda, \quad n = 1, 2. \tag{4.1b}$$

The resulting ordinary differential equations for the Fourier transforms F_1 and F_2 are

$$\frac{dF_1}{dT} = (-\lambda^2 D_1 + i\lambda U_1 - \epsilon\beta_1) F_1 + \epsilon\beta_1 F_2, \tag{4.2a}$$

$$\frac{dF_2}{dT} = (-\lambda^2 D_2 + i\lambda U_1 - \epsilon\beta_2) F_2 + \epsilon\beta_2 F_1, \tag{4.2b}$$

and the initial conditions obtained from (2.12) are

$$F_1(\lambda, 0) = F_2(\lambda, 0) = c_0. \tag{4.2c}$$

Assuming solutions of exponential form

$$F_1(\lambda, T) = P(\lambda)\, e^{r(\lambda)T}, \quad F_2(\lambda, T) = Q(\lambda)\, e^{r(\lambda)T}, \tag{4.3}$$

the characteristic equation of the system (4.2) is found to be

$$[r + m_1(\lambda)]\,[r + m_2(\lambda)] - \epsilon^2 \beta_1 \beta_2 = 0, \tag{4.4}$$

where

$$m_1(\lambda) = \lambda^2 D_1 - i\lambda U_1 + \epsilon\beta_1, \tag{4.5a}$$

$$m_2(\lambda) = \lambda^2 D_2 - i\lambda U_2 + \epsilon\beta_2, \tag{4.5b}$$

and the two solutions of (4.4) are

$$r_{1,2}(\lambda) = -\tfrac{1}{2}(m_1 + m_2) \pm \tfrac{1}{2}[(m_2 - m_1)^2 + 4\epsilon^2 \beta_1 \beta_2]^{\frac{1}{2}}. \tag{4.6}$$

Thus the Fourier transforms satisfying the initial conditions (4.2c) are

$$F_1(\lambda, T) = P_1(\lambda)\, e^{r_1(\lambda)\, T} + P_2(\lambda)\, e^{r_2(\lambda)\, T}, \tag{4.7a}$$

$$F_2(\lambda, T) = [r_1(\lambda)+m_1(\lambda)]\frac{P_1(\lambda)}{\epsilon\beta_1} e^{r_1(\lambda)\, T} + [r_2(\lambda)+m_1(\lambda)]\frac{P_2(\lambda)}{\epsilon\beta_1} e^{r_2(\lambda)\, T}, \tag{4.7b}$$

where
$$P_1(\lambda) = \tfrac{1}{2}c_0\{1+[(m_2-m_1)+2\epsilon\beta_1][(m_2-m_1)^2+4\epsilon^2\beta_1\beta_2]^{-\frac{1}{2}}\}, \tag{4.8a}$$

$$P_2(\lambda) = \tfrac{1}{2}c_0\{1-[(m_2-m_1)+2\epsilon\beta_1][(m_2-m_1)^2+4\epsilon^2\beta_1\beta_2]^{-\frac{1}{2}}\}. \tag{4.8b}$$

Finally, the contaminant concentrations in the fast and slow zones can be determined if the Fourier transforms are inverted. These inverse transformations are

$$c_1(X, T) = \frac{1}{2\pi}\int_{-\infty}^{\infty} P_1(\lambda_1)\exp[Tr_1(\lambda)-\mathrm{i}X\lambda]\,\mathrm{d}\lambda + \frac{1}{2\pi}\int_{-\infty}^{\infty} P_2(\lambda)\exp[Tr_2(\lambda)-\mathrm{i}X\lambda]\,\mathrm{d}\lambda, \tag{4.9a}$$

$$c_2(X, T) = \frac{1}{2\pi}\int_{-\infty}^{\infty} Q_1(\lambda)\exp[Tr_1(\lambda)-\mathrm{i}\lambda X]\,\mathrm{d}\lambda + \frac{1}{2\pi}\int_{-\infty}^{\infty} Q_2(\lambda)\exp[r_2(\lambda)T-\mathrm{i}\lambda X]\,\mathrm{d}\lambda, \tag{4.9b}$$

where

$$Q_1(\lambda) = [r_1(\lambda)+m_1(\lambda)]\frac{P_1(\lambda)}{\epsilon\beta_1}$$

$$= \tfrac{1}{2}c_0\{1-[(m_2-m_1)-2\epsilon\beta_2][(m_2-m_1)^2+4\epsilon^2\beta_1\beta_2]^{-\frac{1}{2}}\}, \tag{4.10a}$$

$$Q_2(\lambda) = [r_2(\lambda)+m_2(\lambda)]\frac{P_2(\lambda)}{\epsilon\beta_1}$$

$$= \tfrac{1}{2}c_0\{1+[(m_2-m_1)-2\epsilon\beta_2][(m_2-m_1)^2+4\epsilon^2\beta_1\beta_2]^{-\frac{1}{2}}\}. \tag{4.10b}$$

If these inversion integrals in (4.9) and (4.10) can be evaluated then the contaminant concentrations will be completely known.

It may be noted that the average contaminant concentration over the entire cross-section including both fast and flow zones is given by

$$c(X, T) = (1-\eta_2)\, c_1(X, T) + \eta_2\, c_2(X, T). \tag{4.11}$$

5. Asymptotically valid inversion

The Fourier inversion integrals in (4.9) are very complicated, as can be seen from the definition of $r_1(\lambda)$, $r_2(\lambda)$, $P_1(\lambda)$ and $P_2(\lambda)$ in (4.5), (4.6) and (4.8). As we are not aware of any method of evaluating these integrals exactly, we shall resort to an asymptotic method which is quite powerful. Specifically, we shall use the saddle-point method (see Copson 1965) to find asymptotic approximations of the integrals, valid for 'large T'. It will later be argued that the approximations are valid even when T is not very large.

Consider the first integral in (4.9a),

$$L_1 = \frac{1}{2\pi}\int_{-\infty}^{\infty} P_1(\lambda)\, e^{Tr_1(\lambda)-\mathrm{i}\lambda X}\,\mathrm{d}\lambda, \tag{5.1}$$

which is to be evaluated along the real axis in the complex λ-plane, with

$$r_1(\lambda) = -\tfrac{1}{2}[m_1(\lambda)+m_2(\lambda)] + \tfrac{1}{2}\{[m_2(\lambda)-m_1(\lambda)]^2+4\epsilon^2\beta_1\beta_2\}^{\frac{1}{2}},$$

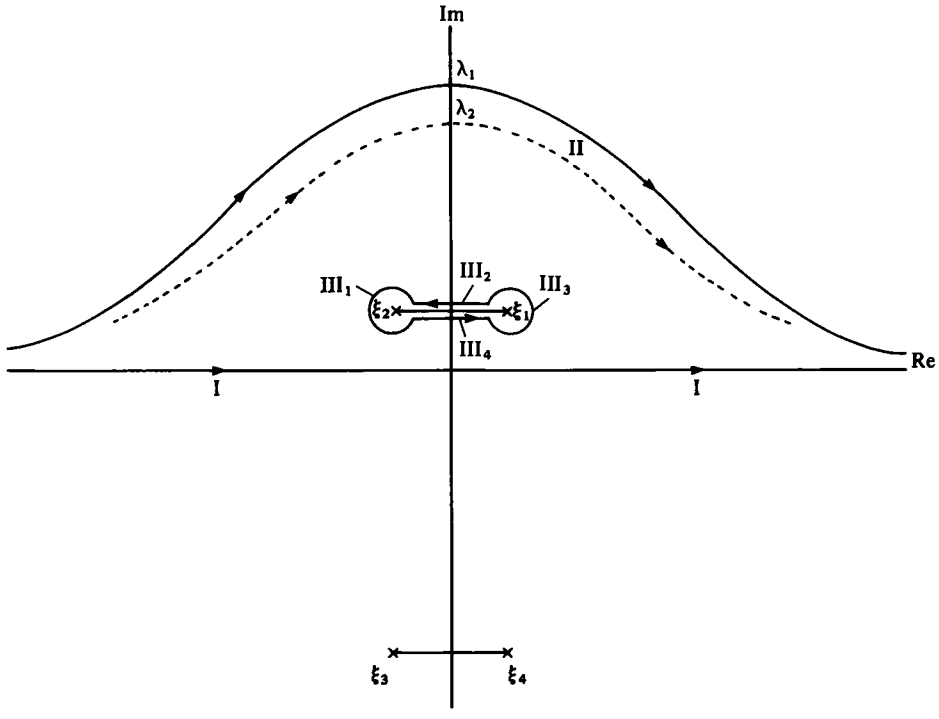

FIGURE 3. Complex λ-plane showing branch points (ξ_1, ξ_2, ξ_3, ξ_4), saddle points (λ_1, λ_2) and contours of integration.

and $m_1(\lambda)$, $m_2(\lambda)$ defined in (4.5). Now the integrand in (5.1) has branch points at the points where

$$[m_1(\lambda)-m_2(\lambda)]^2+4\epsilon^2\beta_1\beta_2 = 0, \tag{5.2}$$

while the exponent $Tr_1(\lambda)$ has saddle points at the points where $\mathrm{d}r_1/\mathrm{d}\lambda = 0$ (see figure 3). If the contour of integration (the real line) can be deformed to pass through the saddle points (path II in figure 3), then the major contributions to the integral will come from the neighbourhood of the saddle points (for 'large T'), and the saddle-point method can be applied to find an asymptotic approximation of the integral.

Similarly, the second integral in (4.9*a*) is

$$L_2 = \frac{1}{2\pi}\int_{-\infty}^{\infty} P_2(\lambda)\, \mathrm{e}^{r_2(\lambda)T-\mathrm{i}\lambda X}\,\mathrm{d}\lambda, \tag{5.3}$$

and this integral has saddle points where $\mathrm{d}r_2/\mathrm{d}\lambda = 0$ and branch points where (5.2) is valid.

However, in deforming a contour from the real line (path I in figure 3) to the path that passes through the saddle point (path II), the integral round the branch cut (path III) must be taken into account.

In the Appendix it is shown that the branch-cut contributions from L_1 and L_2 cancel each other, so that c_1 can be obtained from the saddle-point contributions alone. Similarly the branch-cut contributions from the first and second integrals in (4.9*b*) cancel each other, and c_2 is also obtained from the saddle-point contributions alone.

6. Saddle-point contributions

In (5.1), for large T, the exponent $r_1 T$ has saddle points that satisfy

$$r_1'(\lambda) = -\tfrac{1}{2}(m_1'+m_2')+\frac{(m_2-m_1)(m_2'-m_1')}{2[(m_2-m_1)^2+4\epsilon^2\beta_1\beta_2]^{\frac{1}{2}}} = 0, \tag{6.1}$$

where $(\ )' = \mathrm{d}(\ )/\mathrm{d}\lambda$. Since $\epsilon^2\beta_1\beta_2$ is small ($\epsilon^2\beta_1\beta_2 = O(10^{-1})$) this derivative can be written as a perturbation series in powers of $\epsilon^2\beta_1\beta_2$. Thus

$$r_1'(\lambda) = -m_1'(\lambda)-\frac{\epsilon^2\beta_1\beta_2(m_2'-m_1')}{(m_2-m_1)^2}+3(\epsilon^2\beta_1\beta_2)^2\frac{m_2'-m_1'}{(m_2-m_1)^4}+\ldots. \tag{6.2}$$

Therefore, to the zeroth-order approximation in ϵ (i.e. when $\epsilon = 0$), the saddle point occurs where $m_1'(\lambda) = 0$; that is, where

$$\lambda_1 \approx \mathrm{i}U_1/2D_1.$$

This saddle point will in general occur where

$$\lambda_1 = \frac{\mathrm{i}U_1}{2D_1}+\epsilon q_1+\epsilon^2 q_2+\ldots, \tag{6.3}$$

where $q_1, q_2, \ldots$ can be found by substituting (6.3) in (6.2) and setting the powers of ϵ^j equal to zero for $j = 1, 2, \ldots$. If we limit the expansion to the $O(\epsilon)$ term, we find that the saddle point occurs at

$$\lambda_1 \approx \frac{\mathrm{i}U_1}{2D_1(1+\epsilon^2\beta a_1)}, \tag{6.4a}$$

where

$$a_1 = -\frac{D_2/D_1-U_2/U_1}{[m_2(\lambda_1)-m_1(\lambda_1)]^2} = -\frac{D_2/D_1-U_2/U_1}{[\epsilon(\beta_2-\beta_1)-U_1^2/4D_1(1+D_2/D_1-2U_2/U_1)]^2}. \tag{6.4b}$$

In order to evaluate the integral L_1 by the saddle-point method, we need to know $\mathrm{d}^2r_1/\mathrm{d}\lambda^2$ at $\lambda = \lambda_1$, and by differentiating (6.2) and using (5.8), we find that

$$r_1''(\lambda_1) \approx -2D_1(1-\epsilon^2\beta_1\beta_2 p_1), \tag{6.5a}$$

where

$$p_1 = -\frac{\epsilon(\beta_2-\beta_1)(\Delta_1-1)+(U_1^2/4D_1)(3\Delta_1^3-6\Delta_1\Gamma_1+1-2\Gamma_1+\Gamma_1^2)}{(m_2(\lambda_1)-m_1(\lambda_1))^3}, \tag{6.5b}$$

with $\Delta_1 = D_2/D_1, \Gamma_1 = U_2/U_1$. Also, by expanding (5.2) in powers of $\epsilon^2\beta_1\beta_2$, it is found that

$$r_1(\lambda_1) = -m_1(\lambda_1)+\epsilon^2\beta_1\beta_2[m_2(\lambda_1)-m_1(\lambda_1)]^{-1}-(\epsilon^2\beta_1\beta_2)^4[m_2(\lambda_1)-m_1(\lambda_1)]^{-3}+\ldots. \tag{6.6}$$

Similarly, in the integral L_2 in (5.3), the saddle point for large T occurs where $r_2'(\lambda) = 0$, with

$$r_2(\lambda) = -\tfrac{1}{2}(m_1+m_2)-\tfrac{1}{2}[(m_2-m_1)^2+4\epsilon^2\beta_1\beta_2]^{\frac{1}{2}}. \tag{6.7}$$

Thus it is found that this saddle point occurs at

$$\lambda_2 \approx \frac{\mathrm{i}U_2}{2D_2(1-\epsilon^2\beta_1\beta_2 a_2)}, \tag{6.8a}$$

where

$$a_2 = \frac{D_1/D_2-U_1/U_2}{(m_2(\lambda_2)-m_1(\lambda_2))^2} = \frac{D_1/D_2-U_1/U_2}{[\epsilon(\beta_2-\beta_1)-(U_2^2/4D_2)(2U_1/U_2-D_1/D_2-1)]^2}. \tag{6.8b}$$

Also, at this saddle point

$$r_2''(\lambda_2) \approx -2D_2[1+\epsilon^2\beta_1\beta_2 p_2], \tag{6.9a}$$

where

$$p_2 = -\frac{(U_2^2/4D_2)\,(3\Delta_2^2-6\Delta_2\Gamma_2+1-2\Gamma_2+\Gamma_2^2)+\epsilon(\beta_2-\beta_1)\,(1-\Delta_2)}{(m_2(\lambda_2)-m_1(\lambda_2))^3}, \tag{6.9b}$$

with $\Delta_2 = D_1/D_2$, $\Gamma_2 = U_1/U_2$, and

$$r_2(\lambda_2) = -m_2(\lambda_2)-\epsilon^2\beta_1\beta_2[m_2(\lambda_2)-m_1(\lambda_2)]^{-1}+(\epsilon^2\beta_1\beta_2)^2\,[m_2(\lambda_2)-m_1(\lambda)]^{-3}+\ldots. \tag{6.10}$$

Thus the behaviour of the exponents in (4.9*a*) near the saddle points has been determined. These integrals in (4.9*a*) can be written as

$$L_n = \frac{1}{2\pi}\int_{-\infty}^{\infty} P_n(\lambda)\,\mathrm{e}^{Tr_n(\lambda)-\mathrm{i}\lambda X}\,\mathrm{d}\lambda, \quad n = 1,2. \tag{6.11}$$

Near the saddle points $r_n'(\lambda_n) = 0$, and we may write, using the Taylor series for $r_n(\lambda)$ about $\lambda = \lambda_n$,

$$r_n(\lambda) = r_n(\lambda_n)+\tfrac{1}{2}r_n''(\lambda_n)\,(\lambda-\lambda_n)^2+\ldots. \tag{6.12}$$

Thus (6.11) becomes, using only the first term in the Taylor series for $P_n(\lambda)$ about $\lambda = \lambda_n$,

$$L_n \sim \frac{1}{2\pi}\int_{-\infty}^{\infty} P_n(\lambda_n)\exp\{Tr_n(\lambda_n)-\mathrm{i}\lambda_n X-\tfrac{1}{2}T[-r_n''(\lambda_n)]\,\sigma_n^2-\mathrm{i}\sigma_n X\}\,\mathrm{d}\sigma_n,$$

where

$$\sigma_n = \lambda-\lambda_n, \quad n = 1,2. \tag{6.13}$$

Thus

$$L_n \sim \frac{P_n(\lambda_n)}{2\pi}\exp\left[-\mathrm{i}\lambda_n X+Tr_n(\lambda_n)-\frac{X^2}{2T(-r_n''(\lambda_n))}\right]$$

$$\times\int_{-\infty}^{\infty}\exp\left\{\tfrac{1}{2}T(-r_n''(\lambda))\left[\sigma_n+\frac{\mathrm{i}X}{T(-r_n''(\lambda_n))}\right]^2\right\}\mathrm{d}\sigma_n, \quad n = 1,2. \tag{6.14}$$

The integral in (6.14) is a standard integral, and the result is

$$L_n \sim \frac{P_n(\lambda_n)}{\{2\pi T(-r_n''(\lambda_n))\}^{\frac{1}{2}}}\exp\left\{-\mathrm{i}\lambda_n X+Tr_n(\lambda_n)-\frac{X^2}{2T(-r_n''(\lambda_n))}\right\}.$$

This can be rearranged to give the first term in the asymptotic expansion of the integral as

$$L_n \sim \frac{P_n(\lambda_n)}{\{2\pi T(-r_n''(\lambda_n))\}^{\frac{1}{2}}}\exp\left\{-\frac{[X-\mathrm{i}\lambda_n r_n''(\lambda_n)\,T]^2}{2T(-r_n''(\lambda_n))}+[r_n(\lambda_n)+\tfrac{1}{2}\lambda_n^2 r_n''(\lambda_n)]\,T\right\}, \quad n = 1,2. \tag{6.15}$$

The first terms in the asymptotic expansions of the saddle-point contributions to the integrals involved in the inversion for $c_1(X,T)$ have now been obtained. These expansions (6.15) also apply to the integrals in (4.9*b*) for $c_2(X,T)$, provided that $P_n(\lambda_n)$ is replaced with $Q_n(\lambda_n)$, $n = 1,2$. Higher-order terms in the asymptotic expansions can be obtained (see Carrier, Krook & Pearson 1966), but it will be shown that these first terms give quite accurate results.

It may be noted that the expansion of $P_n(\lambda_n)$ and $Q_n(\lambda_n)$, $n = 1, 2$, in powers of ϵ using (4.8) and (4.10) gives, to $O(\epsilon^2)$,

$$P_1(\lambda_1) = c_0(1-\epsilon\beta_1 b_1), \quad P_2(\lambda_2) = c_0\,\epsilon\beta_1 b_2, \tag{6.16a,b}$$

$$Q_1(\lambda_1) = c_0\,\epsilon\beta_2 w_1, \qquad Q_2(\lambda_2) = c_0(1-\epsilon\beta_2 w_2), \tag{6.17a,b}$$

where

$$b_1 = \frac{1}{n_1}+\frac{\epsilon\beta_2}{n_1^2}, \quad w_1 = \frac{1}{n_1}+\frac{\epsilon\beta_1}{n_1^2}, \tag{6.18a}$$

$$b_2 = \frac{1}{n_2}+\frac{\epsilon\beta_2}{n_2^2}, \quad w_2 = \frac{1}{n_2}+\frac{\epsilon\beta_1}{n_n^2}, \tag{6.18b}$$

with

$$n_1 = m_1(\lambda_1)-m_2(\lambda_1) = \frac{U_1^2}{4D_1}\left(1+\frac{D_2}{D_1}-\frac{2U_2}{U_1}\right)-\epsilon(\beta_2-\beta_1), \tag{6.19a}$$

$$n_2 = m_1(\lambda_2)-m_2(\lambda_2) = \frac{U_2^2}{4D_2}\left(\frac{2U_1}{U_2}-\frac{D_1}{D_2}-1\right)-\epsilon(\beta_2-\beta_1). \tag{6.19b}$$

The 'large-T' asymptotic behaviour of the saddle-point contributions to the contaminant concentrations $c_1(X, T)$, $c_2(X, T)$ can now be determined. Thus, putting (6.15) in (4.9a) and making use of (6.4), (6.5), (6.6), (6.8), (6.9) and (6.10) for λ_n, $r_n(\lambda_n)$ and $r_n''(\lambda_n)$ $(n = 1, 2)$, it is found that for the fast zone, to $O(\epsilon^2)$,

$$\begin{aligned}
&c_1(X,T)\\
&\sim P_1(\lambda_1)\,[4\pi D_1 T(1-\epsilon^2 Bp_1)]^{-\frac{1}{2}}\exp\left\{-\frac{[X-U_1(1+\epsilon^2 Ba_1)\,(1-\epsilon^2 Bp_1)\,T]^2}{4TD_1(1-\epsilon^2 Bp_1)}\right.\\
&\left.+\left[-\frac{U_1^2}{4D_1}(1+\epsilon^4 B^2 a_1^2)-\epsilon\beta_1+\frac{\epsilon^2 B}{m_2(\lambda_1)-m_1(\lambda_1)}+\frac{U_1^2}{4D_1}(1+\epsilon^2 Ba_1)^2\,(1-\epsilon^2 Bp_1)\right]\right\}\\
&+P_2(\lambda_2)\,[4\pi D_2 T(1+\epsilon^2 Bp_2)]^{-\frac{1}{2}}\exp\left\{-\frac{[X-U_2(1-\epsilon^2 Ba_2)\,(1+\epsilon^2 Bp_2)\,T]^2}{4TD_2(1+\epsilon^2 Bp_2)}\right.\\
&\left.+T\left[-\frac{U_2^2}{4D_2}(1+\epsilon^4 B^2 a_2^2)-\epsilon\beta_2-\frac{\epsilon^2 B}{m_2(\lambda_2)-m_1(\lambda_1)}+\frac{U_2^2}{4D_2}(1-\epsilon^2 Ba_2)^2\,(1+\epsilon^2 Bp_2)\right]\right\},
\end{aligned} \tag{6.20}$$

where $B = \beta_1\beta_2$.

This expression can be simplified, using (6.16) for $P_n(\lambda_n)$ and keeping only terms of order ϵ^2, giving

$$\begin{aligned}
c_1(X,T) &\sim c_0(1-\epsilon\beta_1 b_1)\,[4\pi D_1 T(1-\epsilon^2 Bp_1)]^{-\frac{1}{2}}\exp\left\{-\frac{[X-U_1(1+\epsilon^2 B(a_1-p_1))\,T]^2}{4TD_1(1-\epsilon^2 Bp_1)}\right.\\
&\left.-T\left[\epsilon\beta_1+\epsilon^2 B\left(\frac{1}{n_1(\lambda_1)}-\frac{U_1^2}{4D_1}(2a_1-p_1)\right)\right]\right\}\\
&+c_0\,\epsilon\beta_1 b_2[4\pi D_2 T(1+\epsilon^2 Bp_2)]^{-\frac{1}{2}}\exp\left\{-\frac{[X-U_2(1-\epsilon^2 B(a_2-p_2))\,T]^2}{4TD_2(1+\epsilon^2 Bp_2)}\right.\\
&\left.-T\left[\epsilon\beta_2-\epsilon^2 B\left(\frac{1}{n_2(\lambda_2)}+\frac{U_2^2}{4D_2}(2a_2-p_2)\right)\right]\right\}.
\end{aligned} \tag{6.21}$$

A similar asymptotically valid expression can be obtained for the saddle-point contribution to the slow-zone concentration by simply replacing P_1 and P_2 in (6.20) with Q_1 and Q_2. Thus, if we define

$$\phi_1(X,T) = [4\pi D_1 T(1-\epsilon^2 B p_1)]^{-\frac{1}{2}} \exp\left\{-\frac{[X-U_1(1+\epsilon^2 B(a_1-p_1))\,T]^2}{4TD_1(1-\epsilon^2 B p_1)} - T\left[\epsilon\beta_1+\epsilon^2 B\left(\frac{1}{n_1(\lambda_1)}-\frac{U_1^2}{4D_1}(2a_1-p_1)\right)\right]\right\}, \quad (6.22a)$$

$$\phi_2(X,T) = [4\pi D_2 T(1+\epsilon^2 B p_2)]^{-\frac{1}{2}} \exp\left\{-\frac{[X-U_2(1-\epsilon^2 B(a_2-p_2))\,T]^2}{4TD_2(1+\epsilon^2 B p_2)} - T\left[\epsilon\beta_2-\epsilon^2 B\left(\frac{1}{n_2(\lambda_2)}+\frac{U_2^2}{4D_2}(2a_2-p_2)\right)\right]\right\}, \quad (6.22b)$$

then, in the slow zone,

$$c_2(X,T) \sim c_0\epsilon\beta_2 w_1 \phi_1(X,T) + c_0(1-\epsilon\beta_2 w_2)\phi_2(X,T). \quad (6.23)$$

Finally, the saddle-point contribution to the average contaminant concentration over the entire cross-section, $c(X,T)$, is found by using (6.21) and (6.23) in (4.10). The result is

$$c(X,T) \sim c_0[(1-\eta_2)(1-\epsilon\beta_1 b_1)+\eta_2\epsilon\beta_2 w_1]\phi_1(X,T) + c_0[(1-\eta_2)\epsilon\beta_1 b_2+\eta_2(1-\epsilon\beta_2 w_2)]\phi_2(X,T). \quad (6.24)$$

While these expressions for $c_1(X,T)$, $c_2(X,T)$ and $c(X,T)$ are in principle valid for 'large T', experience with asymptotically valid expressions shows that they will be valid even when T is not very large (see Carrier *et al.* 1966, p. 242). This will be especially true in this case where ϵ is small and the expressions are exactly valid for all time when $\epsilon = 0$. Thus we anticipate that these expressions will be useful even when T is as small as 2 or 3. In principle, the higher-order terms in the asymptotic expression can be obtained, but these first terms are sufficient to show the main results.

Since ϵ^2 is very small, (6.21)–(6.24) for c_1, c_2 and c can be written approximately as

$$c_1(X,T) \sim (4\pi D_1 T)^{-\frac{1}{2}} \exp\left[-\frac{(X-U_1 T)^2}{4D_1 T}-\epsilon\beta_1 T\right], \quad (6.25a)$$

$$c_2(X,T) \sim (4\pi D_2 T)^{-\frac{1}{2}} \exp\left[-\frac{(X-U_2 T^2)^2}{4D_2 T}-\epsilon\beta_2 T\right], \quad (6.25b)$$

$$c(X,T) = \eta_1 c_1(X,T)+\eta_2 c_2(X,T). \quad (6.25c)$$

7. Comparison with experimental data

7.1. *Decay rate of peak concentration*

In the first stage of his three-stage description (i.e. for $0.5 < T < 4$) Sullivan (1971) observed from his experiments that the depth-averaged concentration c consisted of a Gaussian distribution followed by a long tail. The peak value of the Gaussian was observed to decay at the rate

$$\exp(-0.3T), \quad (7.1)$$

which is faster than the $T^{-\frac{1}{2}}$ decay rate predicted by the Taylor model.

From (6.22) and (6.24) our theory predicts that the peak value of the bulk concentration (which at small times is the same as the peak value of the leading Gaussian) will decay approximately at the rate

$$T^{-\frac{1}{2}} \exp(-\epsilon\beta_1 T). \tag{7.2}$$

Using the inverse fractional depth $\beta_1 = 1.582$ from (11.11) and $\epsilon = 0.137$ from (3.14), it is found that $\epsilon\beta_1 = 0.22$. Also, in the range $1.5 < T < 6$ the approximation $T^{-\frac{1}{2}} \approx \exp(-0.17T)$ is valid. Thus the overall decay rate of the peak concentration as predicted by our theory is

$$\begin{aligned} T^{-\frac{1}{2}} \exp(-\epsilon\beta_1 T) &\approx \exp(-0.17T) \exp(-0.22T) \\ &= \exp(-0.39T). \end{aligned} \tag{7.3}$$

This is close to but slightly higher than the rate observed experimentally by Sullivan (1971) and given in (7.1) above.

7.2. *Comparison with concentration data*

For the comparison of the predictions of our theory with the experimentally measured variation of the depth-averaged concentration c with X at a fixed time, we shall use the experiments of Sullivan (1971). Specifically, the last row of data in his table 2 had $R_* = U_* h/\nu = 790$ (where ν is the kinematic viscosity of the fluid),

$$h = 7.32 \text{ cm}, \quad u_* = 1.21 \text{ cm/s}, \quad u = 22.9 \text{ cm/s}, \quad U = 18.926 \quad \text{and} \quad \epsilon = 0.133$$

(and therefore $\kappa = 3\epsilon = 0.4$). For the optimal choice of fractional depths given in (11.11), (3.4a,b) give an average fast-zone velocity $U_1 = 20.38$ and slow-zone velocity $U_2 = 16.43$. Similarly, the values $D_1 = 0.26$ and $D_2 = 2.08$ are obtained from (3.8a). The calculated value of U_1/U is 1.08, compared with the experimental value of 1.125.

For this case then, the fast-zone, slow-zone and average contaminant concentrations (c_1, c_2, c) predicted by the theory (6.21)–(6.24)) are plotted in figures 4(a) (for $T = 1.0$) and 4(b) (for $T = 2$). The curves for c are quite similar to the experimental observations of Sullivan (1971) in the first stage of the dispersion process.

While our theory could be compared with the excellent experimental data of Fischer (1966), such comparisons would not be meaningful, since most of Fischer's data were obtained in the second stage of the dispersion process, while the theory presented so far is useful only for the first stage.

There are five main facts that can be observed from (6.21)–(6.24) and figure 4. These five findings are important analytical results of this paper, and distinguish our results from most previous work on dispersion in open channels and streams. They are the following.

(i) For small and moderate times from release of contaminant, the contaminant distribution in the fast zone consists of a forward Gaussian cloud whose peak value is $O(1)$ and which travels at speed $\approx U_1$, followed by a small Gaussian cloud whose peak value is $O(\epsilon)$ and which travels at speed $\approx U_2$. In the slow zone the main cloud is the slow one whose peak value is $O(1)$ and which travels at speed $\approx U_2$, preceded by a small Gaussian cloud whose peak value is $O(\epsilon)$ and which travels at speed $\approx U_1$.

(ii) The depth-averaged contaminant concentration $c(X, T)$ consists of a leading Gaussian distribution mostly (but not completely) in the fast zone and a trailing Gaussian distribution mostly (but not completely) in the slow zone. Because $D_2 > D_1$ the trailing Gaussian distribution will disperse longitudinally faster than the leading one, and will thus form the long tail that is characteristic of the early stage of all dispersion observations in open channels.

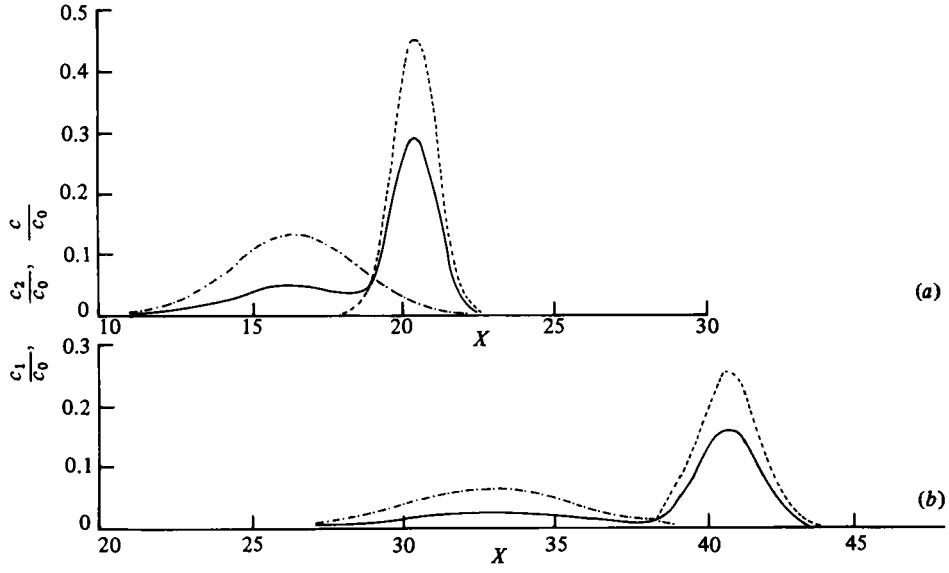

FIGURE 4. Theoretically predicted fast-zone (- - - - - - -), slow-zone (—·—·) and average (——) contaminant concentrations given by equations (6.21)–(6.24) plotted against X at (*a*) $T = 1$ and (*b*) $T = 2$, with $U_1 = 20.38$, $U_2 = 16.43$, $U = 18.93$, $D_1 = 0.26$, $D_2 = 2.08$, $\eta_2 = 0.3679$, $\eta_1 = 0.6321$ and $\epsilon = 0.133$.

(iii) In both the fast and slow zones the peak value of the leading Gaussian cloud decays exponentially like $T^{-\frac{1}{2}} \exp(-\epsilon\beta_1 T)$, while the peak value of the trailing Gaussian cloud decays exponentially like $T^{-\frac{1}{2}} \exp(-\epsilon\beta_2 T)$. With the slow zone thinner than the fast zone ($\beta_2 > \beta_1$), the trailing Gaussian cloud therefore decays faster than the leading one. Thus for reasonably small times the peak value of the average concentration $c(X, T)$ decays exponentially with time; this exponential decay was observed by Sullivan (1971) in his experiments, and we have shown that the $T^{-\frac{1}{2}} \exp(-\epsilon\beta_1 T)$ rate of decay obtained from our analysis is close to the rate observed by Sullivan.

(iv) The theoretically calculated value of the non-dimensional diffusivity of the leading Gaussian distribution, $D_1 = 0.016/\kappa^3$ (≈ 0.24), is consistent with the range of values of $0.1 < D_1 < 0.3$, which were found experimentally by Sullivan in the first stage of the dispersion process.

(v) The theoretically calculated value of the non-dimensional lateral diffusivity between the fast and slow zones, $\epsilon = \frac{1}{3}\kappa$ (≈ 0.137) is in agreement with the value of 0.12 found experimentally by Sullivan (1971) for the average lateral diffusivity.

However, there is a difficulty with these asymptotic solutions obtained using the saddle-point method ((6.21)–(6.24)). Because of the exponential decay of the peak values of both the leading and trailing Gaussian distributions, it is clear that $\int_{-\infty}^{\infty} c(X, T)\,\mathrm{d}X$ will decay exponentially with time, and thus violates the conservation of contaminant mass. While the approximation has been shown to be useful for small times, it cannot be correct at large times.

In order to resolve this question, we shall in the next few sections obtain and analyse an exact solution of the slow-zone model for the case $D_1 = D_2$. It will be shown that the exponential decay of the peak value of the contaminant distribution applies only at fairly small times. At large times this exact solution approaches a single Gaussian distribution which travels at the bulk speed U in accordance with the Taylor model.

8. Reformulation of the Fourier integrals

The Fourier-transform solutions given in (4.9) and (4.10) for c_1 and c_2 can be written in a more compact form in terms of two Fourier-inversion integrals. Thus let

$$A(\lambda) = [(m_2-m_1)^2+4\epsilon^2\beta_1\beta_2]^{\frac{1}{2}}$$
$$= \{[\lambda^2(D_2-D_1)+\mathrm{i}\lambda(U_1-U_2)+\epsilon(\beta_2-\beta_1)]^2+4\epsilon^2\beta_1\beta_2\}^{\frac{1}{2}}, \tag{8.1a}$$

$$q_+(X,T) = \frac{1}{2\pi}\int_{-\infty}^{\infty} A^{-1}(\lambda)\exp[-\mathrm{i}\lambda X-\tfrac{1}{2}T(m_1+m_2-A)]\,\mathrm{d}\lambda, \tag{8.1b}$$

$$q_-(X,T) = \frac{1}{2\pi}\int_{-\infty}^{\infty} A^{-1}(\lambda)\exp[-\mathrm{i}\lambda X-\tfrac{1}{2}T(m_1+m_2+A)]\,\mathrm{d}\lambda, \tag{8.1c}$$

with
$$m_1+m_2 = \lambda^2(D_1+D_2)-\mathrm{i}\lambda(U_1+U_2)+\epsilon(\beta_1+\beta_2). \tag{8.2}$$

It is then pleasantly surprising that c_1 and c_2 can be written simply in terms of the derivatives of q_+ and q_-; thus

$$c_1(X,T) = c_0[\partial_T-D_2\partial_X^2+U_2\partial_X+\epsilon(\beta_1+\beta_2)](q_+-q_-), \tag{8.3a}$$

$$c_2(X,T) = c_0[\partial_T-D_1\partial_X^2+U_1\partial X+\epsilon(\beta_1+\beta_2)](q_+-q_-), \tag{8.3b}$$

$$c(X,T) = c_0[\partial_T-(\eta_1 D_2+\eta_2 D_1)\partial_X^2+(\eta_1 U_2+\eta_2 U_1)\partial_X+\epsilon(\beta_1+\beta_2)](q_+-q_-). \tag{8.3c}$$

It may also be noted from (8.1) that

$$q(X,T) = q_+-q_- = \frac{1}{\pi}\int_{-\infty}^{\infty} A^{-1}(\lambda)\exp[-\mathrm{i}\lambda X-\tfrac{1}{2}T(m_1+m_2)]\sinh[\tfrac{1}{2}A(\lambda)T]\,\mathrm{d}\lambda. \tag{8.4}$$

The telegraph equation

The aim of this subsection is to point out the similarities and differences between our two-layer model and the two-layer model given by Smith's (1982) telegraph equation. The coupled dispersion equations (2.7) can be combined into a single *fourth-order* partial differential equation for the bulk concentration as follows:

$$\partial_T^2 c+D_1D_2\partial_X^4 c-(D_1+D_2)\partial_{TXX}^3 c-(U_1D_2+U_2D_1)\partial_X^3 c$$
$$+[U_1U_2-\epsilon(\beta_1D_2+\beta_2D_1)]\partial_X^2 c+(U_1+U_2)\partial_{XT}^2 c+\epsilon\beta_1\beta_2\partial_T c+\epsilon\beta_1\beta_2 U\partial_X c = 0, \tag{8.5}$$

where we have used the facts that

$$\beta_1+\beta_2 = \beta_1\beta_2, \tag{8.6a}$$

$$\beta_1 U_2+\beta_2 U_1 = \beta_1\beta_2 U. \tag{8.6b}$$

On the other hand Smith's (1982) telegraph equation for the two-layer model is (using dimensionless variables),

$$(\partial_T+v_0\partial_X+\mu)(\partial_T+U\partial_X-\bar{\kappa}\partial_X^2)c-\mu D_\ell(\infty)\partial_X^2 c = 0. \tag{8.7}$$

This equation can be written as a *third-order* partial differential equation

$$\partial_T^2 c-\bar{\kappa}\partial_{TXX}^3 c-v_0\bar{\kappa}\partial_X^3 c+[v_0U-\mu(\bar{\kappa}+D_\ell(\infty))]\partial_X^2 c$$
$$+(v_0+U)\partial_{TX}^2+\mu\partial_T c+\mu U\partial_X c = 0. \tag{8.8}$$

The two equations agree when $D_1 = D_2 = \bar{\kappa} = 0$, provided that

$$\mu = \epsilon\beta_1\beta_2, \quad D_\ell(\infty) = \frac{(U_1-U_2)^2}{\epsilon(\beta_1\beta_2)^2}, \tag{8.9a,b}$$

$$v_0 = \eta_2 U_1 + \eta_1 U_2, \tag{8.9c}$$

$$v_0 - U = -(U_1-U_2)\frac{\beta_2-\beta_1}{\beta_1\beta_2}.$$

However, when $D_1 \neq 0$, $D_2 \neq 0$, $\bar{\kappa} \neq 0$, the two equations are not the same, since our (8.5) is fourth-order and Smith's (8.8) is third-order.

9. Exact solution when $D_1 = D_2$.

An exact solution of the slow-zone model of dispersion can be found in the form of a convolution integral in the special case when $D_1 = D_2$ (Thacker 1976). In this section this exact solution will be obtained, and then its behaviour will be explored for small times and large times from the release of the contaminant.

Let $D_1 = D_2 = D_0$, then the expression (8.1*a*) for $A(\lambda)$ becomes much simpler and can be written as

$$\begin{aligned} A(\lambda) &= [-\lambda^2(U_1-U_2)^2 + 2i\epsilon\lambda(U_1-U_2)(\beta_2-\beta_1) + \epsilon^2(\beta_2+\beta_1)^2]^{\frac{1}{2}} \\ &= (U_1-U_2)[(i\lambda+d)(i\lambda+b)]^{\frac{1}{2}}, \end{aligned} \tag{9.1a}$$

where

$$d = \frac{\epsilon(\beta_2-\beta_1)}{U_1-U_2} - \frac{2i\epsilon(\beta_1+\beta_2)^{\frac{1}{2}}}{U_1-U_2}, \tag{9.1b}$$

$$b = \frac{\epsilon(\beta_2-\beta_1)}{U_1-U_2} + \frac{2i\epsilon(\beta_1+\beta_2)^{\frac{1}{2}}}{U_1-U_2}, \tag{9.1c}$$

and we have used the fact that $\beta_1+\beta_2 = \beta_1\beta_2$. Equation (8.4) for q can in this case be written as

$$\begin{aligned} q(X,T) = \frac{1}{\pi}(U_1-U_2)^{-1}\exp[-\tfrac{1}{2}\epsilon(\beta_1+\beta_2)T]\int_{-\infty}^{\infty}[(i\lambda+d)(i\lambda+b)]^{-\frac{1}{2}} \\ \times\exp(-i\lambda G - \lambda^2 D_0 T)\sinh\{\tfrac{1}{2}[(i\lambda+d)(i\lambda+b)]^{\frac{1}{2}}T(U_1-U_2)\}\,d\lambda, \end{aligned} \tag{9.2}$$

where

$$G = X - \tfrac{1}{2}T(U_1+U_2). \tag{9.3}$$

$q(X,T)$ is the Fourier inverse of the product of two Fourier transforms, and so can be written as a convolution. Thus, from Campbell & Forster (1961, p. 113),

$$\begin{aligned} &\frac{1}{2\pi}\int_{-\infty}^{\infty}[(i\lambda+d)(i\lambda+b)]^{-\frac{1}{2}}\exp(-i\lambda G)\sinh\{\tfrac{1}{2}[(i\lambda+d)(i\lambda+b)]^{\frac{1}{2}}T(U_1-U_2)\}\,d\lambda \\ &\quad = \tfrac{1}{2}\exp[\tfrac{1}{2}(d+b)G]\,J_0\{\tfrac{1}{2}[\tfrac{1}{4}T^2(U_1-U_2)^2 - G^2]^{\frac{1}{2}}(d-b)\} \\ &\quad = \tfrac{1}{2}\exp\left[\frac{\epsilon(\beta_2-\beta_1)G}{U_1-U_2}\right] I_0\left\{\tfrac{1}{4}[T^2(U_1-U_2)^2 - G^2]^{\frac{1}{2}}\frac{2\epsilon(\beta_1\beta_2)^{\frac{1}{2}}}{U_1-U_2}\right\}, \\ &\qquad\qquad G < |\tfrac{1}{2}T(U_1-U_2)|, \end{aligned} \tag{9.4}$$

where J_0 and I_0 are respectively the Bessel function and the modified Bessel function of the first kind, of zero order, and we have used the fact that $J_0(-iR) = I_0(R)$. Also,

$$\frac{1}{2\pi}\int_{-\infty}^{\infty}\exp(-i\lambda G - \lambda^2 D_0 T)\,d\lambda = (4\pi D_0 T)^{-\frac{1}{2}}\exp\left(-\frac{G^2}{4D_0 T}\right). \tag{9.5}$$

Equation (9.2) for $q(X, T)$ can therefore be written as the following convolution integral:

$$q(X,T) = (4\pi D_0 T)^{-\frac{1}{2}}(U_1-U_2)^{-1}\exp(-\tfrac{1}{2}\epsilon\beta_1\beta_2 T)\int_{-g(T)}^{g(T)} I_0(R)\exp H\,\mathrm{d}\xi, \quad (9.6a)$$

where

$$H = -\frac{[X-\frac{1}{2}(U_1+U_2)T-\xi]^2}{4D_0T}+\frac{\epsilon(\beta_2-\beta_1)\xi}{U_1-U_2}, \quad (9.6b)$$

$$R = \left[\frac{2\epsilon(\beta_1\beta_2)^{\frac{1}{2}}}{U_1-U_2}\right][\tfrac{1}{4}T^2(U_1-U_2)^2-\xi^2]^{\frac{1}{2}}, \quad (9.6c)$$

$$g(T) = \tfrac{1}{2}T(U_1-U_2). \quad (9.6d)$$

Equations (9.6) can then be used in (8.3) to calculate the contaminant concentrations c_1, c_2 and c as functions of X and T. The exact solution of the slow-zone model for the case $D_1 = D_2 = D_0$ has thus been obtained. The result is

$$\begin{aligned} c_{1,2} = {} & (\tfrac{1}{2}c_0(4\pi D_0T)^{-\frac{1}{2}}\left\{\exp\left(-\frac{G_1^2}{4D_0T}-\epsilon\beta_1T\right)+\exp\left(-\frac{G_2^2}{4D_0T}-\epsilon\beta_2T\right)\right. \\ & \pm 2\exp(-\tfrac{1}{2}\epsilon\beta_1\beta_2T)\int_{-g(T)}^{g(T)}\left[\frac{G-\xi}{4DT}\right]I_0(R)\exp H\,\mathrm{d}\xi \\ & +\frac{\epsilon\beta_1\beta_2}{U_1-U_2}\exp(-\tfrac{1}{2}\epsilon\beta_1\beta_2T)\int_{-g(T)}^{g(T)} I_0(R)\exp H\,\mathrm{d}\xi \\ & \left.+\frac{2\epsilon^2\beta_1\beta_2T}{U_1-U_2}\exp(-\tfrac{1}{2}\epsilon\beta_1\beta_2T)\int_{-g(T)}^{g(T)}\frac{I_0'(R)}{R}\exp H\,\mathrm{d}\xi\right\}, \end{aligned} \quad (9.7a)$$

where

$$G_1 = X-U_1T, \quad (9.7b)$$

$$G_2 = X-U_2T, \quad (9.7c)$$

and in the second line of (9.7a) c_1 has the positive sign while c_2 has the negative sign. Finally, c is obtained from the equation $c = \eta_1 c_1+\eta_2 c_2$. These solutions reduce to the solution given by Smith (1982) in the non-diffusive case $D_1 = D_2 = 0$.

Although the convolution integrals can be evaluated numerically, we shall instead seek to find asymptotically valid explicit expressions for the contaminant concentrations for small T and for large T.

10. Exact solution valid for small T

The maximum value of the argument of the modified Bessel function $I_0(R)$ in (9.7a) occurs when $\xi = 0$, and is $R = \epsilon T(\beta_1\beta_2)^{\frac{1}{2}}$. Thus when T is small the argument will be small and the ascending series for the modified Bessel function can be used, that is (Abramowitz & Stegun 1965),

$$I_0(R) = 1+\tfrac{1}{4}R^2+(\tfrac{1}{4}R^2)^2/(2!)^2+\ldots, \quad (10.1a)$$

$$\frac{I_0'(R)}{R} = \frac{I_1(R)}{R} = \tfrac{1}{2}+\tfrac{1}{4}(\tfrac{1}{4}R^2)+\ldots. \quad (10.1b)$$

In order to obtain a first approximation for the contaminant concentrations, the first terms in (10.1) can be used, i.e. $I_0(R) \approx 1$, thus neglecting terms that are $O(\epsilon^2T^2)$. In this case the integrals in (9.7a) can be evaluated in terms of error functions. The last

integral in (9.7*a*) can be neglected since it is $O(\epsilon^2 T)$, and the first and second integrals can be rewritten using the change of variable (from ξ to ζ)

$$\zeta(4D_0T)^{\frac{1}{2}} = \xi - \left[G + \frac{2\epsilon(\beta_2-\beta_1)D_0T}{U_1-U_2}\right]. \tag{10.2}$$

The resulting expressions for the contaminant concentration in the fast zone is (for small T)

$$c_1 \approx c_0(4\pi D_0T)^{-\frac{1}{2}}\exp\left(\frac{-G_1^2}{4D_0T} - \epsilon\beta_1 T\right) - \tfrac{1}{2}c_0\epsilon\beta_1 M, \tag{10.3a}$$

where

$$M = (U_1-U_2)^{-1}\exp\left[-\tfrac{1}{2}\epsilon\beta_1\beta_2 T + \frac{\epsilon(\beta_2-\beta_1)G}{U_1-U_2} + \frac{\epsilon^2 D_0 T(\beta_2-\beta_1)^2}{(U_1-U_2)^2}\right]$$
$$\times\left\{\operatorname{erf}\left[\frac{G_1+E}{(4D_0T)^{\frac{1}{2}}}\right] - \operatorname{erf}\left[\frac{G_2+E}{(4D_0T)^{\frac{1}{2}}}\right]\right\}, \tag{10.3b}$$

and

$$E = \frac{2\epsilon T D_0(\beta_2-\beta_1)}{U_1-U_2}. \tag{10.3c}$$

with erf as the error function. Similarly, the contaminant concentration in the slow zone is (for small T)

$$c_2 \approx c_0(4\pi D_0T)^{-\frac{1}{2}}\exp\left(-\frac{G_2^2}{4D_0T} - \epsilon\beta_2 T\right) - \tfrac{1}{2}\epsilon c_0\beta_2 M, \tag{10.4}$$

while the depth-averaged contaminant concentration is (for small T)

$$c \approx c_0(4\pi D_0T)^{-\frac{1}{2}}\left[\eta_1\exp\left(-\frac{G_1^2}{4D_0T} - \epsilon\beta_1 T\right) + \eta_2\exp\left(-\frac{G_2^2}{4D_0T} - \epsilon\beta_2 T\right)\right] - \epsilon c_0 M. \tag{10.5}$$

These expressions for the contaminant concentrations will be useful so long as $\frac{1}{4}\epsilon^2\beta_1\beta_2 T^2$ is small ($O(\epsilon)$). For $\beta_1 \approx \beta_2 \approx 2$, this will be valid for $0 \leqslant T \leqslant 3.0$, or approximately for the first stage of the dispersion process (Sullivan 1971).

The significance of (10.3)–(10.5) is that we have confirmed from an exact solution that the asymptotic results obtained using the saddle-point method (§6) are approximately correct for the first stage of the dispersion process. There are differences, but these differences are small ($O(\epsilon)$) and may arise because of different ways of writing an asymptotic series. Most significantly the exponential rate of decay has been confirmed from an exact solution, and the average contaminant concentration consists primarily of a leading Gaussian and a trailing Gaussian.

The condition $D_1 = D_2$ under which the exact solution was obtained is not a good model of the physical situation in which $D_2 > D_1$. Therefore these exact results will not be compared with experimental concentration–time data.

11. Exact solution valid for large T

When T is large it is convenient to use the longitudinal variable $Z = X - UT$, which moves with the bulk velocity. In (9.6) and (9.7) we also make the change of variable (from ξ to μ),

$$\xi = \mu + T[U - \tfrac{1}{2}(U_1+U_2)] = \mu + \frac{T(U_1-U_2)(\beta_2-\beta_1)}{2\beta_1\beta_2}, \tag{11.1}$$

and use the fact that

$$\beta_1+\beta_2-\frac{(\beta_2-\beta_1)^2}{2\beta_1\beta_2}=4. \tag{11.2}$$

Equation (9.6a) for q can then be written as

$$q(Z,T)=(U_1-U_2)^{-1}(4\pi D_0T)^{-\frac{1}{2}}\exp(-2\epsilon T)\times\int_{-g(T)/\beta_1}^{g(T)/\beta_2}\exp\left[-\frac{(Z-\mu)^2}{4D_0T}+\frac{\epsilon\mu(\beta_2-\beta_1)}{U_1-U_2}\right]I_0(R)\,\mathrm{d}\mu, \tag{11.3a}$$

where

$$R=2\epsilon\left[T^2-\frac{\mu T(\beta_2-\beta_1)}{U_1-U_2}-\frac{\mu^2\beta_1\beta_2}{(U_1-U_2)^2}\right]^{\frac{1}{2}}. \tag{11.3b}$$

The dominant part of the Bessel function in (11.3a) comes from near $R=\epsilon T(\beta_1\beta_2)^{\frac{1}{2}}$. Thus for large T, R is large and we can use the asymptotic expression for the modified Bessel function for large arguments:

$$I_0(R)\sim(2\pi R)^{-\frac{1}{2}}\exp R. \tag{11.4}$$

Using (11.3b), $I_0(R)$ can be written as

$$I_0\sim(4\pi\epsilon T)^{-\frac{1}{2}}\exp\left[2\epsilon T-\frac{\mu(\beta_2-\beta_1)}{U_1-U_2}-\frac{\mu^2(\beta_1\beta_2)^2}{4\epsilon T(U_1-U_2)^2}\right]. \tag{11.5}$$

Equation (11.5) can now be used in (11.3a), and the asymptotic result for q is

$$q(Z,T)\sim c_0\epsilon^{-1}[(4\pi TD_0)(4\pi TD_\ell(\infty))]^{-\frac{1}{2}}\int_{-\infty}^{\infty}\exp\left[-\frac{(Z-\mu)^2}{4D_0T}-\frac{\mu^2}{4D_\ell(\infty)T}\right]\mathrm{d}\mu, \tag{11.6}$$

where

$$D_\ell(\infty)=\frac{(U_1-U_2)^2}{\epsilon(\beta_1\beta_2)^2} \tag{11.7}$$

is the contribution to the longitudinal dispersion coefficient at large times due purely to the lateral mixing. Since the convolution of two Gaussian distributions is another Gaussian distribution, the asymptotic result is

$$q(Z,T)\sim\frac{c_0\,\mathrm{e}^{-Z^2/4D(\infty)T}}{\epsilon\beta_1\beta_2(4\pi D(\infty)T)^{\frac{1}{2}}}, \tag{11.8a}$$

where

$$D(\infty)=D_\ell(\infty)+D_0 \tag{11.8b}$$

is the overall longitudinal dispersion coefficient at large times (for this case in which $D_1=D_2=D_0$). Finally, when (11.8) is used in (8.3), it is found that the fast-zone, slow-zone and average contaminant concentrations all approach the same asymptotic limit, which is

$$c(X,T)\sim\frac{c_0\exp\left[-\frac{(X-UT)^2}{4D(\infty)T}\right]}{(4\pi D(\infty)T)^{\frac{1}{2}}}. \tag{11.9}$$

Two significant results have thus been obtained from the behaviour of the exact solution at large times:

(i) the contaminant distribution asymptotically approaches a Gaussian distribution travelling with the bulk speed U at large times, as predicted by the Taylor model;

(ii) the overall longitudinal-dispersion coefficient at large times consists of the diffusivity D_0 plus a contribution $D_\ell(\infty)$ which depends entirely on the lateral mixing.

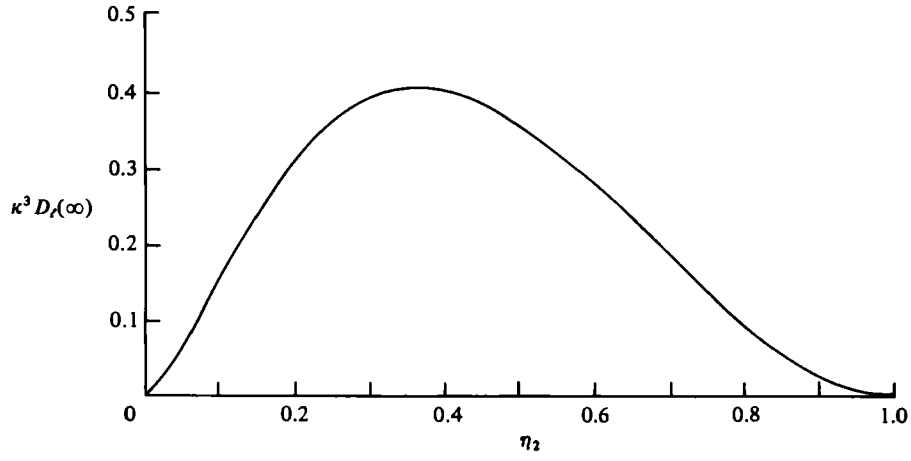

FIGURE 5. Theoretically predicted dispersion coefficient at large times ($\kappa^3 D_\ell(\infty)$) due to lateral mixing, plotted as a function of the slow-zone fractional depth η_2.

The magnitude of $D(\infty)$ and the optimal choice of zonal fractional depths

Equation (11.7) for $D_\ell(\infty)$ can be simplified if we use (3.4*a*,*b*) for U_1 and U_2 and equation (3.14) for ϵ. The result is

$$D_\ell(\infty) = 3(\eta_2 \ln \eta_2)^2/\kappa^3. \tag{11.10}$$

In figure 5, $\kappa^3 D_\ell(\infty)$ is plotted as a function of η_2. The maximum value of $D_\ell(\infty)$ can be found at the point where $\mathrm{d}D_\ell(\infty)/\mathrm{d}\eta_2 = 0$. This calculation shows that the maximum occurs when

$$\eta_2 = \mathrm{e}^{-1} = 0.3679; \quad \eta_1 = 1 - \mathrm{e}^{-1} = 0.6321, \tag{11.11}$$

These are therefore the optimal choices of the fractional depths, and the resulting maximum value of $D_\ell(\infty)$ is

$$D_\ell(\infty) = 0.4060/\kappa^3. \tag{11.12}$$

This is almost the same as the longitudinal dispersion coefficient calculated by Elder (1959) ($D = 0.4041/\kappa^3$) and based on the lateral diffusivity ϵ_y. It may be noted that the optimal choices of fractional depths given in (11.11) are close to but different from the values given by Smith (1982), i.e. $\eta_2 = 0.3276$, $\eta_1 = 0.6724$.

Using (11.12) in (11.8*b*), it is found that the overall longitudinal dispersion coefficient at large times is given by

$$D(\infty) = 0.406/\kappa^3 + D_0. \tag{11.13}$$

This result has been obtained for the case $D_1 = D_2 = D_0$. We may, however, approximate the average diffusivity across the channel in the more general case ($D_1 \neq D_2$) by using

$$\begin{aligned} D_0 &\approx \eta_1 D_1 + \eta_2 D_2 \\ &= 0.048/\kappa^3, \end{aligned} \tag{11.14}$$

where we have used the values of D_1 and D_2 calculated in (3.8*a*) and the optimal fractional depths from (11.11). The final result is

$$D(\infty) = 0.454/\kappa^3. \tag{11.15}$$

If $\kappa = 0.41$ then $D(\infty) = 6.6$. This value of $D(\infty)$ is higher than Elder's (1959), and is exactly the value suggested by Chatwin (1971, p. 696) for Sullivan's second stage on the basis of an analysis of Fischer's (1966) experimental data.

Finally, it is important to determine the values of T for which these large-time asymptotic results are valid. The asymptotic expression given in (11.4) for the modified Bessel function $I_0(R)$ is good to within 5% error when $R > 3$. Since the dominant part of $I_0(R)$ comes from near $R = \epsilon T(\beta_1 \beta_2)^{\frac{1}{2}}$, this implies that the large-time asymptotic results obtained in this section are good when

$$T > \frac{3}{2\epsilon} = \frac{9}{2\kappa},$$

that is

$$T > 11, \quad \text{for } \kappa = 0.41.$$

(At $R = 1$ ($T \approx 4$) the asymptotic expression for $I_0(R)$ is in error by about 20%.) Since we have neglected the viscosity-dominated layer, this estimate of T is the time required for the contaminant to sample fully the flow variation outside the viscous layer. Thus our asymptotic results are useful for Sullivan's second stage. This is consistent with the results of Dewey & Sullivan (1977), who showed that in turbulent flow in a smooth pipe the Gaussian distribution for c is approached when $T > 300$. This would be the time required for the contaminant to sample the entire flow, including the viscous layer, and thus giving Sullivan's third stage.

12. Conclusion

The principal analytical results of this paper have been stated in §§7 and 11. Significant results which are consistent with experimental data have been obtained for the first and second stages of the dispersion process. The viscous layer has been neglected, but it should be possible to include this layer in future work using a three-zonal model. The exact solution that we analysed is valid only when $D_1 = D_2$, whereas §3 shows that $D_2 > D_1$. The effects of this zonal difference in diffusivity on the exact solution will be explored in subsequent work. In addition, the slow zone can be formulated to include the regions of slow flow along the sides of the channel. The inclusion of these slow regions may help to explain why Fischer (1966) found that the longitudinal-dispersion coefficient is significantly increased when the sides of the channel are rough (thus leading to a thicker slow zone). It is also clear that the slow-zone model can be applied to pipe flow (both turbulent and laminar) and to plane Poiseuille flow. These applications will be presented elsewhere.

Finally, it is pertinent to point out that in this paper the boundary between the fast and slow zones is not associated with any drastic change in the properties of the flow. Rather, the slow-zone model is meant to present a simple (first) approximation of the phenomenon of longitudinal dispersion resulting from (i) velocity differences over the cross-section, and (ii) transverse exchange. The two zones with two different velocities U_1 and U_2 can be regarded as the simplest possible discretization of the full velocity profile. As Thacker (1976) has noted, better approximations (especially at small times) can be obtained if three or more zones are used. It is, however, remarkable that so much useful information can be obtained from the simple two-zone model.

At the time this paper was first submitted for publication the authors were not aware of the work of Thacker (1976) and Smith (1981, 1982) on two-zone models. The first author wishes to thank the referees for pointing out these references and for all their useful comments, all of which helped the thought process that sharpened this paper into a self-consistent piece of work.

Appendix

We wish to show here that the values of the Fourier-inversion integrals (4.9*a*,*b*) remain unchanged when the contour of integration is changed from the real line to contours that pass through the saddle points. These saddle points λ_1 and λ_2 are given by (6.4*a*) and (6.8*a*) and lie on the positive imaginary axis as shown in figure 3. From (4.8) let

$$P_1(\lambda) = \frac{1}{2}\left[1-\frac{f(\lambda)}{g_1^{\frac{1}{2}}(\lambda)}\right]c_0, \tag{A 1}$$

$$P_2(\lambda) = \frac{1}{2}\left[1-\frac{f(\lambda)}{g_1^{\frac{1}{2}}(\lambda)}\right]c_0, \tag{A 2}$$

where
$$f(\lambda) = m_2(\lambda)-m_1(\lambda)+2\epsilon\beta_1, \tag{A 3}$$

$$g_1(\lambda) = (m_1-m_2)^2+4\epsilon^2\beta_1\beta_2 = [\lambda^2(D_1-D_2)-\mathrm{i}\lambda(U_1-U_2)+\epsilon(\beta_1-\beta_2)]^2+4\epsilon^2\beta_1\beta_2. \tag{A 4}$$

Equation (4.9*a*) can then be written in the form

$$c_1(X,T) = \frac{1}{2\pi}\int_{-\infty}^{\infty}\left[\left(1+\frac{f}{g_1^{\frac{1}{2}}}\right)\exp\tfrac{1}{2}g_1^{\frac{1}{2}}+\left(1-\frac{f}{g_1^{\frac{1}{2}}}\right)\exp\left(-\tfrac{1}{2}g_1^{\frac{1}{2}}\right)\right] \times\exp\left[-\mathrm{i}\lambda X-\tfrac{1}{2}(m_1-m_2)\,T\right]\mathrm{d}\lambda, \tag{A 5}$$

or

$$c_1(X,T) = \frac{1}{2\pi}\int_{-\infty}^{\infty}2\left[\cosh\tfrac{1}{2}g_1^{\frac{1}{2}}+\frac{f}{g_1^{\frac{1}{2}}}\sinh\tfrac{1}{2}g_1^{\frac{1}{2}}\right]\exp\left[-\mathrm{i}\lambda X-\tfrac{1}{2}(m_1+m_2)\,T\right]\mathrm{d}\lambda. \tag{A 6}$$

In this integral the branch points occur at the zeros of $g_1(\lambda)$, i.e.

$$m(\lambda) = \pm 2\mathrm{i}\epsilon\,(\beta_1\beta_2)^{\frac{1}{2}}, \tag{A 7}$$

with
$$m(\lambda) = \lambda^2(D_1-D_2)-\mathrm{i}\lambda(U_1-U_2)+\epsilon(\beta_1-\beta_2). \tag{A 8}$$

Thus the branch points occur at the four points

$$\lambda = \xi_{1,2,3,4} = -\left\{\frac{\mathrm{i}(U_1-U_2)}{2(D_2-D_1)}\right\}\left\{1+\left[1-\frac{4\epsilon(D_2-D_1)\,(\beta_1-\beta_2\pm 2\mathrm{i}(\beta_1\beta_2)^{\frac{1}{2}}}{(U_1-U_2)^2}\right]^{\frac{1}{2}}\right\}, \quad D_1\neq D_2. \tag{A 9}$$

For small $\epsilon\beta$ these branch points can be written in pairs as

$$\xi_{3,4} \approx -\frac{\mathrm{i}(U_1-U_2)}{D_2-D_1}+\mathrm{i}\epsilon(\beta_1-\beta_2\pm\mathrm{i}(\beta_1\beta_2)^{\frac{1}{2}})\,(U_1-U_2)^{-1}, \tag{A 10}$$

$$\xi_{1,2} \approx \frac{\epsilon[\pm 2(\beta_1\beta_2)^{\frac{1}{2}}+\mathrm{i}(\beta_2-\beta_1)]}{U_1-U_2}. \tag{A 11}$$

We can take one branch cut joining ξ_1 and ξ_2 and another branch cut joining ξ_3 and ξ_4, as shown in figure 3. Both ξ_3 and ξ_4 lie well down in the lower half-plane. Thus when the contour of integration is deformed from I (the real line) to II (passing through a saddle point), the branch cut from ξ_3 to ξ_4 is not affected and does not contribute to the integral. Similarly, for $\beta_1<\beta_2$ both ξ_1 and ξ_2 lie in the lower half-plane, and the branch cut joining them does not contribute to the integral.

On the other hand, for $\beta_1>\beta_2$, ξ_1 and ξ_2 both lie near the origin in the upper half-plane, and so the integral round them (contour III in fig. 3) must be considered when we deform the path from I to II. This integral round the branch cut can be

divided into two circular parts (III_1 and III_3 in figure 3) and two straight parts (III_2 and III_4).

The integrals round the circular paths III_1 and III_3 can easily be shown to vanish as the radii of the circles tend to zero. The integral on III_2 is a line integral from ξ_1 to ξ_2. On this line $g_1^{\frac{1}{2}}$ will be positive. On the other hand, on III_4 (the lower side) $g_1^{\frac{1}{2}}$ will be negative. Thus $\cosh \frac{1}{2}g_1^{\frac{1}{2}} + (f/g_1^{\frac{1}{2}}) \sinh \frac{1}{2}g_1^{\frac{1}{2}}$ does not change sign when we move from III_2 to III_4. Therefore the integrals on III_2 and III_4 will cancel, since one is the line integral from ξ_1 to ξ_2 and the other is the line integral from ξ_2 to ξ_1 of the same integrand.

We have thus shown that the Fourier-inversion integral for $c_1(X, T)$ round the contour III vanishes, and so we can deform the path of integration from the real line I to the contour II which passes through the saddle point. From (4.9*b*) the Fourier-inversion integral for $c_2(X, T)$ can be similarly deformed.

REFERENCES

Abramowitz, M. & Stegun, I. A. 1968 *Handbook of Mathematical Functions*. Dover.

Aris, R. 1956 On the dispersion of solute in fluid flowing through a tube. *Proc. R. Soc. Lond.* A **235**, 67–77.

Campbell, G. A. & Foster, R. M. 1948 *Fourier Integrals for Practical Applications*. Van Nostrand.

Carrier, C. F., Krook, M. & Pearson, C. E. 1966 *Functions of a Complex Variable*. McGraw-Hill.

Chatwin, P. C. 1971 On the interpretation of some longitudinal dispersion experiments. *J. Fluid Mech.* **48**, 689–702.

Chatwin, P. C. 1973 A calculation illustrating the effects of the viscous sub-layer on longitudinal dispersion. *Q. J. Mech. Appl. Maths* **26**, 427–439.

Chatwin, P. C. & Sullivan, P. J. 1982 The effect of aspect ratio on longitudinal diffusivity in rectangular channels. *J. Fluid Mech.* **120**, 347–358.

Copson, E. T. 1965 *Asymptotic Expansions*. Cambridge University Press.

Dewey, R. & Sullivan, P. J. 1977 The asymptotic stage of longitudinal turbulent dispersion within a tube. *J. Fluid Mech.* **80**, 293–303.

Elder, J. W. 1959 The dispersion of marked fluid in turbulent shear flow. *J. Fluid Mech.* **5**, 544–560.

Fischer, H. B. 1966 Longitudinal dispersion in laboratory and natural streams. Ph.D. thesis published in *Rep.* KH-R-12, *Keck Lab., Pasadena, California*.

Fischer, H. B. 1973 Longitudinal dispersion and turbulent mixing in open channel flow. *Ann. Rev. Fluid Mech.* **5**, 59–78.

Hays, J. R. 1966 Mass transport mechanisms in open channel flow. Ph.D. thesis, Vanderbilt University, Nashville, Tennessee.

Jobson, H. E. & Sayre, W. W. 1970 *J. Hydraul. Div. ASCE* **96**, 703–24.

Smith, R. 1979 Calculation of shear-dispersion coefficients. In *Mathematical Modelling of Turbulent Diffusion in the Environment* (ed. C. J. Harris), pp. 343–362.

Smith, R. 1981 A delay–diffusion description for contaminant dispersion. *J. Fluid Mech.* **105**, 469–486.

Smith, R. 1982 Non-uniform discharges of contaminants in shear flows. *J. Fluid Mech.* **120**, 71–89.

Sullivan, P. J. 1971 Longitudinal dispersion within a two-dimensional turbulent shear flow. *J. Fluid Mech.* **49**, 551–576.

Taylor, G. I. 1953 Dispersion of soluble matter in solvent flowing slowly through a tube. *Proc. R. Soc. Lond.* A **219**, 196–203.

Taylor, G. I. 1954 The dispersion of matter in turbulent flow through a pipe. *Proc. R. Soc. Lond.* A **223**, 446–468.

Thacker, W. C. 1976 A soluble model of 'shear dispersion'. *J. Phys. Oceanogr.* **6**, 66–75.